		PSA level			
		< 0.5 µg/L	0.5 - 3.5 µg/L	> 3.5 µg/L	
^{18}F-DCFPyL	pos.	1	15	11	19
	neg.	7	2	2	5
^{68}Ga-PSMA	pos.	1	23	22	56
	neg.	8	12	2	5
		prostatectomy			radio-therapy

SUPPLEMENTAL TABLE 1. Absolute numbers of relapsed patients detected with PSMA-PET imaging. The table displays the absolute number of PET-positive (pos.) and PET-negative (neg.) scans acquired with either ^{18}F-DCFPyL (top) or ^{68}Ga-PSMA-HBED-CC (bottom, ^{68}Ga-PSMA). BCR patients received either surgery (left) or radiotherapy (right) as their initial therapy. For prostatectomy patients (left), numbers are shown separately for PSA levels <0.5µg/L (left), PSA levels >3.5µg/L (right) and PSA values within the diagnostic window (0.5-3.5µg/L, middle).

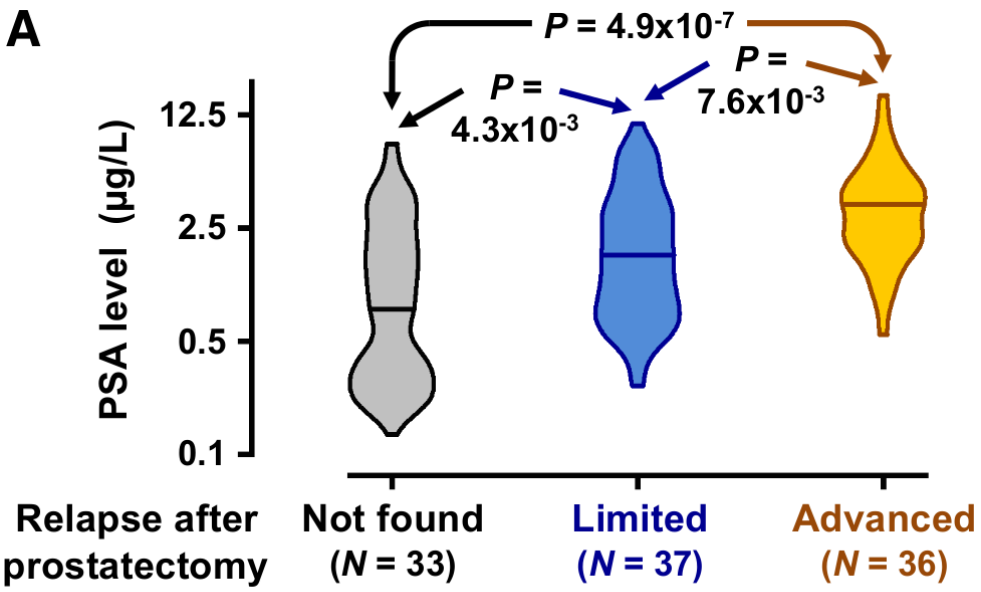

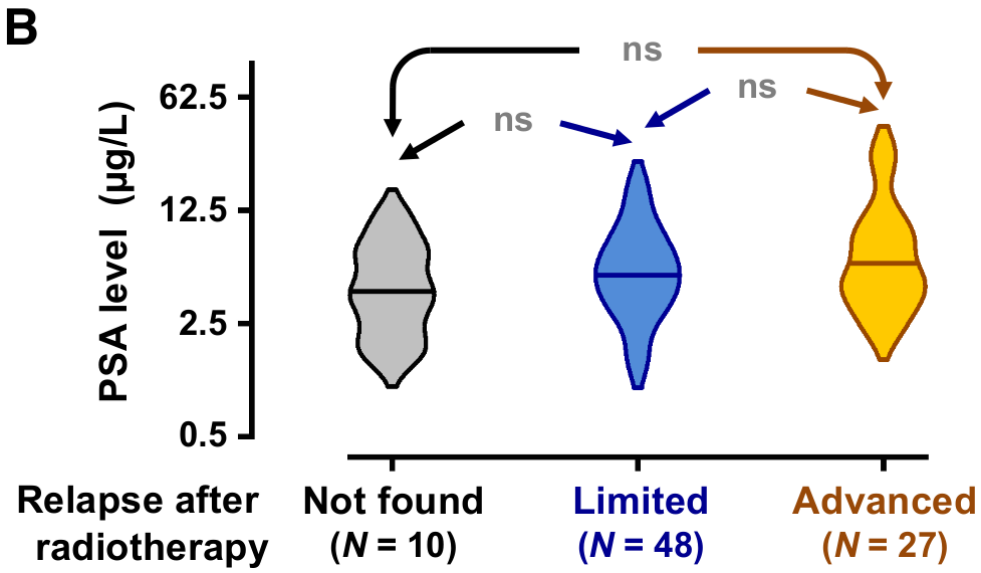

SUPPLEMENTAL FIGURE 1. PSA levels differ significantly at different stages of prostate cancer relapse after surgery. PET scans were split into three groups for patients after prostatectomy (*N*=106, A) and radiotherapy (*N*=85, B). The first group contained all scans, which did not display any PSMA-positive lesions (*not found*, gray). Images, which displayed tumor relapse, were subdivided into scans

with a recurrent tumor at limited stage (*limited*, blue), i.e. local recurrence or infiltration into locoregional lymph nodes, and scans which displayed a recurrent tumor at an advanced stage (*advanced*, orange). Violin plots display the distribution of log-transformed PSA levels (y-axis) for each of these groups (kernel density estimation (KDE), using the probability density function of the normal distribution). Group medians are indicated by vertical bars. Significance values were calculated by two-tailed unpaired heteroscedastic t-tests.

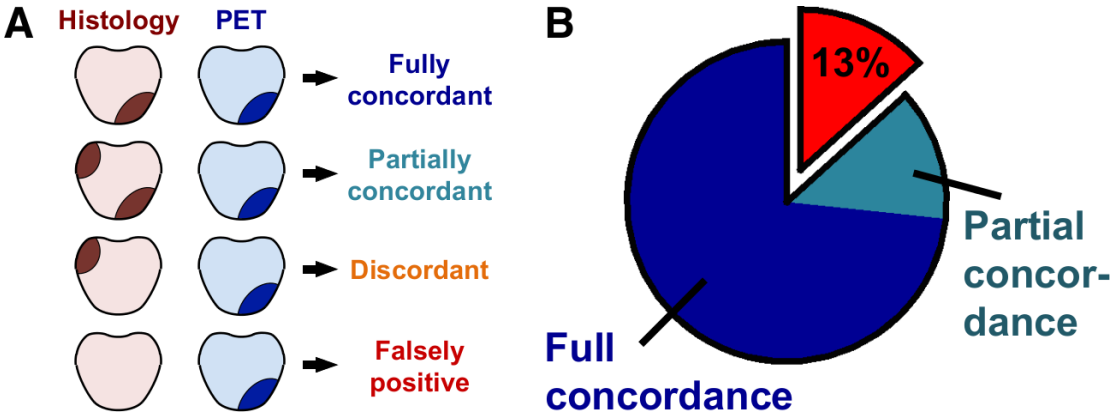

SUPPLEMENTAL FIGURE 2. Histological confirmation of PET-positive lesions. (A) We systematically examined tumor infiltration in the prostate fossa, based on 12 biopsies per patient. Based on these histology results, we compared for each segment tumor infiltration (red, left) with PSMA-positivity in in the corresponding PET scan (blue, right). That way, we differentiated between four different patterns of concordance / discordance. (B) The pie chart displays the fractions of fully (blue) and partially (cyan) concordant cases. Further, falsely positive cases are shown in red, for which PSA-positive lesions lacked histological confirmation.

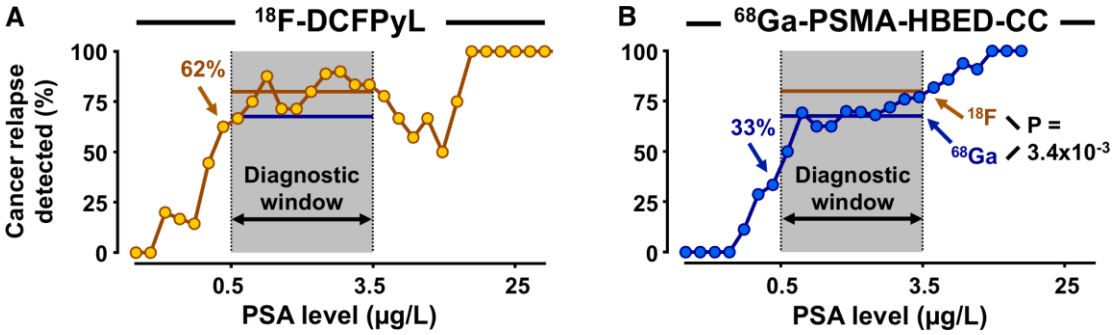

SUPPLEMENTAL FIGURE 3. A PSA-stratified comparison of tracer sensitivity between ^{18}F-DCFPyL and ^{68}Ga-PSMA-HBED-CC. In analogy to the sensitivity curve shown in Figure 1A for prostatectomy patients, PSA-stratified sensitivity curves were plotted separately for prostatectomy patients, examined with ^{18}F-DCFPyL (A, orange) or ^{68}Ga-PSMA-HBED-CC (B, blue), respectively. This analysis revealed discrete but robust differences between both tracer sensitivity curves. The *diagnostic window*, derived from Figures 1A and 1B, is plotted in gray. Arrows indicate point-sensitivity rates for PSA levels ranging around 0.45 µg/L (33% vs. 62%). Vertical lines display curve averages between 0.5 and 3.5 µg/L for ^{68}Ga-PSMA-HBED-CC (blue) and ^{18}F-DCFPyL (orange). Curve averages were compared by two-tailed t-tests.

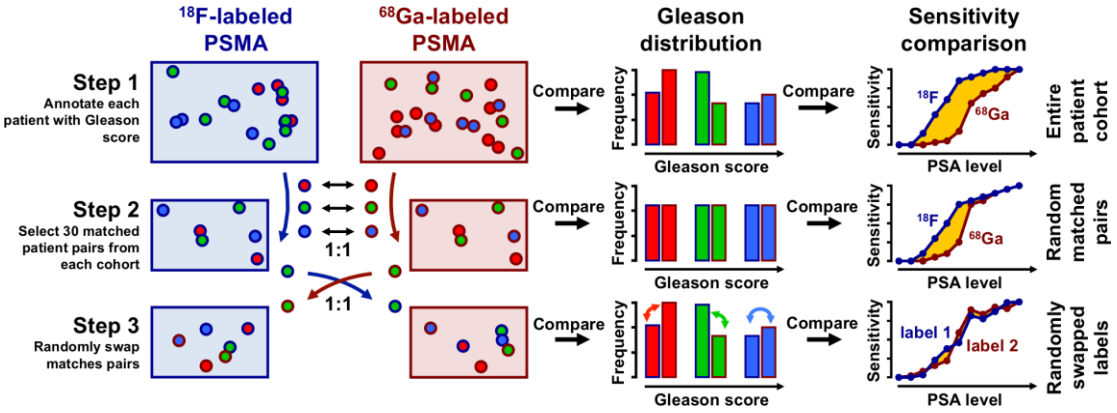

SUPPLEMENTAL FIGURE 4. A Gleason-matched pair analysis of the sensitivity difference between ^{18}F- and ^{68}Ga-labeled PSMA tracers. (A) Schematic representation of the three steps of our Gleason-matched pair analysis. Step 1: In order to correct our comparison between ^{18}F- (blue, left) and ^{68}Ga-labeled (red, right) PSMA tracers for Gleason scores as potential confounders, we first annotated each patient (schematically represented as a dot) with his Gleason score (marked by different colors). Step 2: Secondly, we picked 30 random pairs of patients, from both the ^{18}F and the ^{68}Ga cohort. Each of these patient pairs was chosen with same Gleason score (matched pairs, annotated as 1:1). That way, we obtained subgroups of the ^{18}F and ^{68}Ga cohorts, each containing 30 patients with equal Gleason scores. In parallel to the analyses shown in Figure 1 and Supplemental Figure 3, we plotted cumulative tracer sensitivity curves for both subgroups and compared the PSA-stratified sensitivity. Step 3: Finally, we randomly exchanged matched patient pairs (annotated as 1:1) between the ^{18}F-DCFPyL and ^{68}Ga-PSMA-HBED-CC cohorts. In parallel to step 2, we compared sensitivity between subgroups of both tracer cohorts, which served as a negative control for our confounder correction analysis.

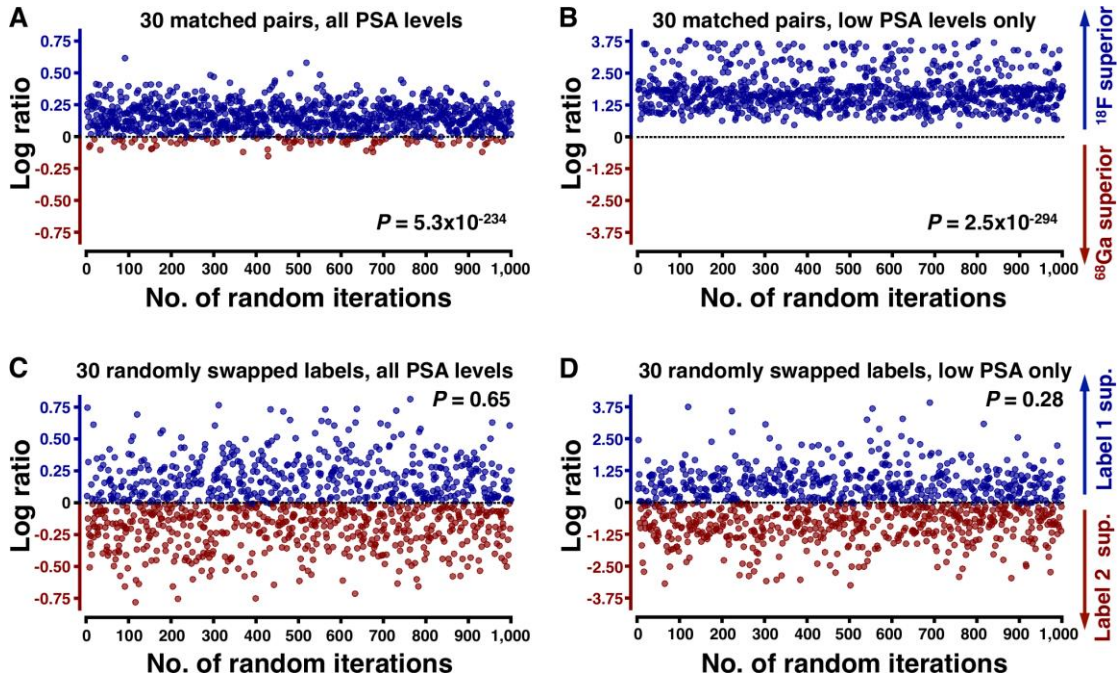

SUPPLEMENTAL FIGURE 5. Correction for Gleason scores preserves sensitivity difference between ^{18}F- and ^{68}Ga-labeled PSMA tracers. (A,B) We performed 1,000 random iterations, in order to derive 1,000 Gleason-matched groups of 30 patients, examined with ^{18}F-DCFPyL or ^{68}Ga-PSMA-HBED-CC, respectively. For each iteration, we calculated the log-transformed ratio between the average sensitivity in the ^{18}F and ^{68}Ga subgroups, respectively. Both of these subgroups shared the same Gleason scores. Ratios are plotted for each iteration, either for the entire range of PSA levels (A) or for PSA values below 1 µg/L (B). Iterations, in which sensitivity of ^{18}F-DCFPyL was superior, are colored in blue (ratio positive), whereas iterations in which ^{68}Ga-PSMA-HBED-CC displayed higher sensitivity are colored in red (ratio negative). The null hypothesis, assuming equal sensitivity between both tracers, is indicated as a dashed line. Significance was derived by comparing the distribution pattern of log-transformed ratios against the null hypothesis.